Supplementary Figures

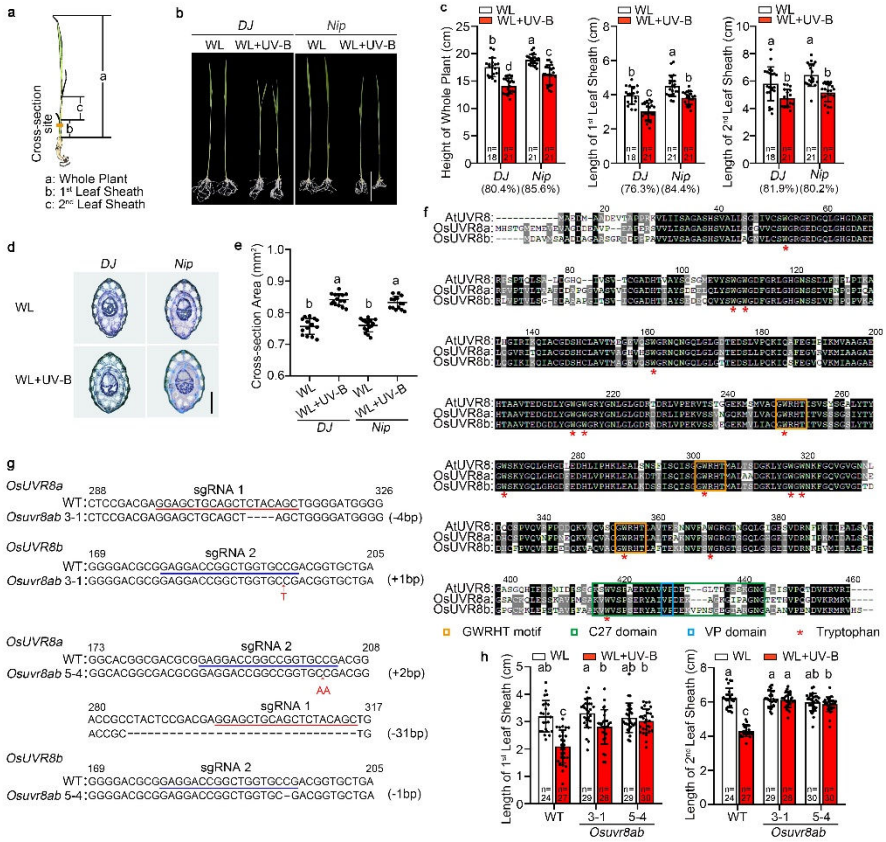

Supplementary Fig. 1 UV-B light results in shorter rice seedlings with thicker stems. a Diagram showing the structure of young rice seedlings. a, whole seedling; b, first leaf sheath; c, second leaf sheath; orange bar, cross-section region. **b** Representative images of 10-day-old wild-type (WT) Dongjin (DJ) and Nipponbare (Nip) seedlings grown under WL or WL+UV-B. Scale bar, 5 cm. **c** Seedling height and lengths of first and second leaf sheaths of the seedlings in **b**. Data are means ± standard deviation (SD). Different lowercase letters indicate statistically significant differences by one-way analysis of variance (ANOVA) followed by Duncan's multiple-range test ($P < 0.05$). **d** Representative images of stem cross sections of DJ and Nip seedlings grown under WL or WL+UV-B. Scale bar, 5 mm. **e** Cross-sectional area of the stems in **d**. Data are means ± SD; $n = 15$. Different lowercase letters indicate statistically significant differences by one-way

ANOVA followed by Duncan's multiple-range test ($P < 0.05$). **f** Protein sequence alignment of AtUVR8 with OsUVR8a and OsUVR8b. Identical residues are highlighted in black, and similar and different residues are highlighted in gray and white, respectively. The positions of tryptophan residues, GWRHT domains, the C27 region and the VP motif are also indicated. **g** Sanger sequencing–based genotyping of two CRISPR/Cas9-generated *Osuvr8a Osuvr8b* (*Osuvr8ab*) homozygous double mutant lines (*Osuvr8ab* 3-1 and *Osuvr8ab* 5-4). The single guide RNA (sgRNA) target site for each gene is underlined, deleted nucleotides are denoted by dashes and inserted nucleotides are shown in red. **h** Lengths of the first and second leaf sheaths of the seedlings in **Fig. 1c**. Data are means ± SD. Different lowercase letters indicate statistically significant differences by one-way ANOVA followed by Duncan's multiple-range test ($P < 0.05$). Source data of Supplementary Figure 1c, e, h are provided as a Source Data file.

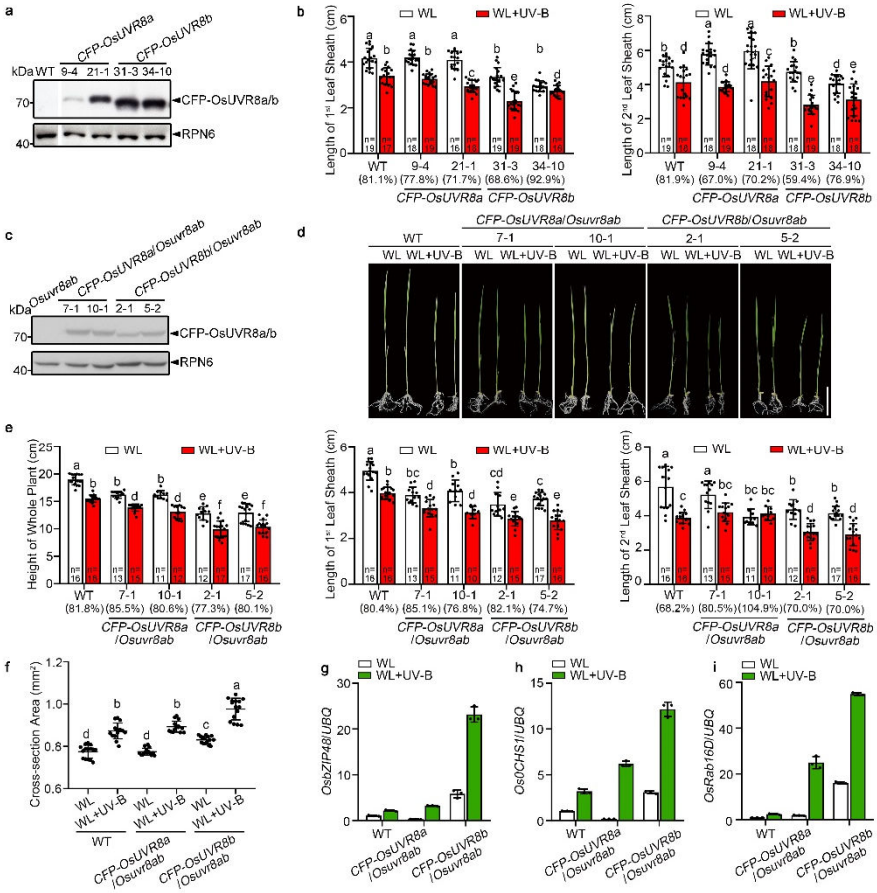

Supplementary Fig. 2 OsUVR8a and OsUVR8b both promote in UV-B response in rice. a Protein levels of transgenic UVR8 in 10-day-old *CFP-OsUVR8a* and *CFP-OsUVR8b* rice seedlings. Immunoblot analysis was performed using an anti-GFP antibodies. Anti-RPN6 was used as a loading control. **b** Length of the first and second leaf sheaths of the seedlings in **Fig. 2a**. Data are means ± SD. Different lowercase letters indicate statistically significant differences by one-way ANOVA followed by Duncan's multiple-range test ($P < 0.05$). **c** Protein levels of transgenic UVR8 in 10-day-old *CFP-OsUVR8a/Osuvr8ab* and *CFP-OsUVR8b/Osuvr8ab* rice seedlings. Immunoblot analysis was performed using an anti-GFP antibodies. Anti-RPN6 was used as a loading control. **d** Representative images of 10-day-old WT DJ, *CFP-OsUVR8a/Osuvr8ab* and *CFP-OsUVR8b/Osuvr8ab* seedlings grown under WL or WL+UV-B. Scale bar, 5 cm. **e** Height of whole plant and

lengths of first and second leaf sheaths of the seedlings in **d.** Data are means ± SD. Different lowercase letters indicate statistically significant differences by one-way ANOVA followed by Duncan's multiple-range test ($P < 0.05$). **f** Cross-sectional area of stems from 10-day-old WT DJ, *CFP-OsUVR8a/Osuvr8ab* and *CFP-OsUVR8b/Osuvr8ab* seedlings. Data are means ± SD; $n = 15$. Different lowercase letters indicate statistically significant differences by one-way ANOVA followed by Duncan's multiple-range test ($P < 0.05$). **g–i** qRT-PCR analysis of the relative transcript levels of *OsbZIP48* (**g**), *OsCHS1* (**h**) and *OsRab16D* (**i**) in WT DJ, *CFP-OsUVR8a/Osuvr8ab* and *CFP-OsUVR8b/Osuvr8ab* seedlings grown under WL or WL+UV-B conditions. qRT-PCR data were normalized to *UBQ*, with the transcript levels in WT DJ under WL set to 1. Data are means ± SD; $n = 3$ biological replicates). Source data of Supplementary Figure 2a-c, e-i are provided as a Source Data file.

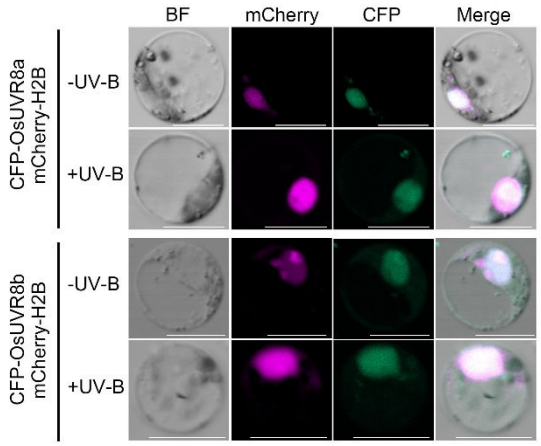

Supplementary Fig. 3 Constitutive nuclear subcellular localization of OsUVR8a and OsUVR8b. Confocal micrographs of protoplasts isolated from WT Nip seedlings. The isolated protoplasts were co-transfected with *mCherry-H2B* and *CFP-OsUVR8a* or *CFP-OsUVR8b*. mCherry-H2B served as a nuclear marker. Scale bars, 10 μm.

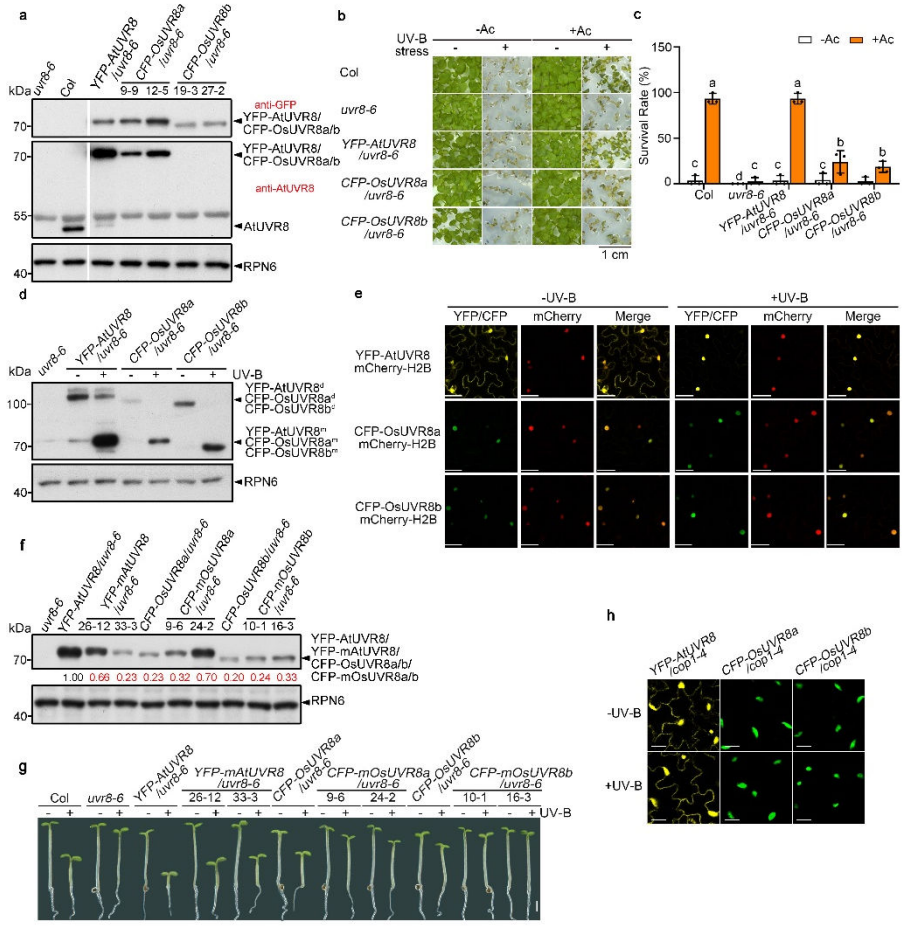

Supplementary Fig. 4 Putative nuclear localization signal in OsUVR8a and OsUVR8b. a Protein levels of UVR8 in 4-day-old Col-0, *uvr8-6*, *YFP-AtUVR8/uvr8-6*, *CFP-OsUVR8a/uvr8-6* and *CFP-OsUVR8b/uvr8-6* seedlings. Immunoblot analysis was performed using anti-GFP and anti-AtUVR8 antibodies. Anti-RPN6 was used as a loading control. **b** Effects of UV-B acclimation and stress treatment in Col-0, *uvr8-6*, *YFP-AtUVR8/uvr8-6*, *CFP-OsUVR8a/uvr8-6* and *CFP-OsUVR8b/uvr8-6*. The seedlings were photographed before and after stress treatment. Scale bar, 1 cm. **c** Survival rate of the seedlings in **b**, quantified after stress treatment and presented as means ± SD; $n = 3$ biological replicates. Different lowercase letters indicate statistically significant differences by one-way ANOVA followed by Duncan's multiple-range test ($P < 0.05$). **d** Conformation of YFP-AtUVR8,

CFP-OsUVR8a and CFP-OsUVR8b in *YFP-AtUVR8/uvr8-6*, *CFP-OsUVR8a/uvr8-6* and *CFP-OsUVR8b/uvr8-6* seedlings grown under −UV-B or +UV-B conditions. Total proteins were assayed by SDS-PAGE without heat denaturation followed by immunoblot analysis using anti-GFP antibodies. Anti-RPN6 was used as a loading control. **e** Confocal micrographs of YFP-AtUVR8, CFP-OsUVR8a and CFP-OsUVR8b subcellular localization in *N. benthamiana*. *N. benthamiana* leaves were co-infiltrated with *mCherry-H2B* and *YFP-AtUVR8*, *CFP-OsUVR8a* or *CFP-OsUVR8b*. Scale bars, 50 μm. **f** Transgenic UVR8 protein levels in 4-day-old *YFP-AtUVR8/uvr8-6*, *YFP-mAtUVR8/uvr8-6*, *CFP-OsUVR8a/uvr8-6*, *CFP-mOsUVR8a/uvr8-6*, *CFP-OsUVR8b/uvr8-6* and *CFP-mOsUVR8b/uvr8-6* seedlings. Immunoblot analysis was performed using anti-GFP antibodies. Anti-RPN6 was used as a loading control. The protein level in *YFP-AtUVR8/uvr8-6* was set as 1. **g** Representative images of 4-day-old Col-0, *uvr8-6*, *YFP-AtUVR8/uvr8-6*, *YFP-mAtUVR8/uvr8-6*, *CFP-OsUVR8a/uvr8-6*, *CFP-mOsUVR8a/uvr8-6*, *CFP-OsUVR8b/uvr8-6* and *CFP-mOsUVR8b/uvr8-6* seedlings grown under −UV-B or +UV-B conditions. Scale bar, 1 mm. **h** Confocal micrographs of YFP-AtUVR8, CFP-OsUVR8a and CFP-OsUVR8b subcellular localization in *YFP-AtUVR8/cop1-4*, *CFP-OsUVR8a/cop1-4* and *CFP-OsUVR8b/cop1-4* seedlings grown under −UV-B or +UV-B conditions. Scale bar, 50 μm. Source data of Supplementary Figure 4a, c, d, f are provided as a Source Data file.

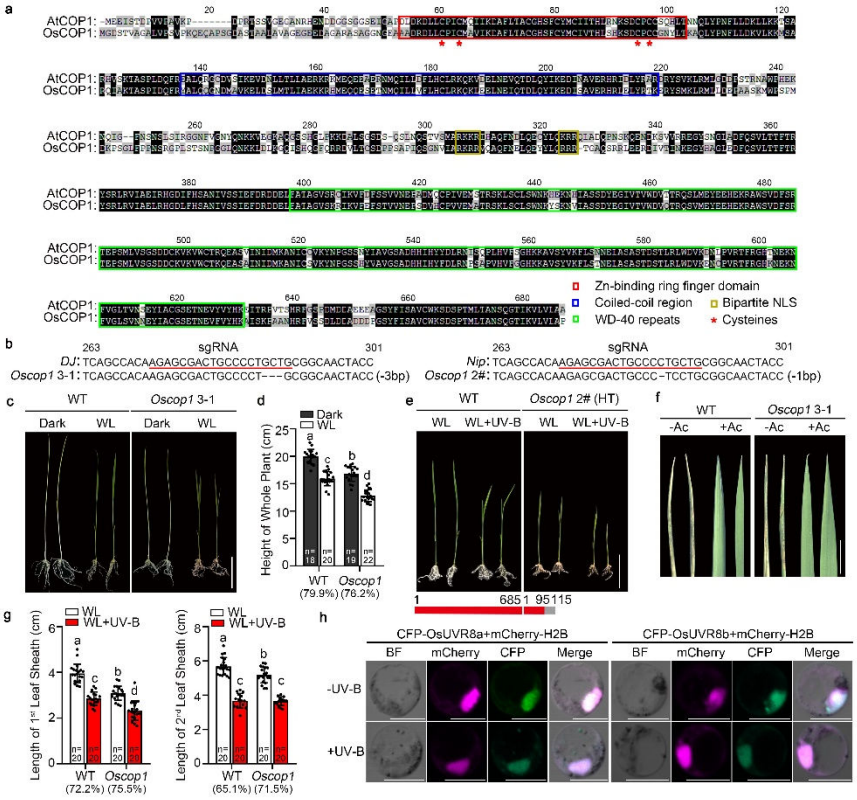

Supplementary Fig. 5 OsCOP1 does not play a positive role in photomorphogenesis in rice. a Protein sequence alignment of AtCOP1 and OsCOP1. Identical residues are highlighted in black, and similar and different residues are highlighted in gray and white, respectively. The positions of the zinc (Zn)-binding ring-finger domain, coiled-coil region, bipartite NLS and WD-40 repeats are also indicated. **b** Sanger-sequencing-based genotyping of the CRISPR/Cas9-generated *Oscop1* mutants. The sgRNA target site is underlined and deleted nucleotides are denoted by dashes. **c** Representative images of WT DJ and *Oscop1* homozygous seedlings grown in darkness or under WL conditions. Scale bar, 5 cm. **d** Height of the seedlings in **c**. Data are means ± SD. Different lowercase letters indicate statistically significant differences by one-way ANOVA followed by Duncan's multiple-range test ($P < 0.05$). **e** Representative images of WT Nip and *Oscop1/OsCOP1* seedlings grown under WL or WL+UV-B conditions. Scale bar, 5 cm. The

diagram below the images indicates the predicted truncated OsCOP1 protein. **f** Representative images of the second leaf from WT DJ and *Oscop1* homozygous seedlings grown under non-acclimated or acclimated conditions before UV-B stress treatment. Scale bar, 2 mm. **g** Length of the first and second leaf sheaths of the seedlings in **Fig. 6a**. Data are means ± SD. Different lowercase letters indicate statistically significant differences by one-way ANOVA followed by Duncan's multiple-range test ($P < 0.05$). **h** Confocal micrographs of protoplasts isolated from *Oscop1* homozygous seedlings. The isolated protoplasts were co-transfected with *mCherry-H2B* and *CFP-OsUVR8a* or *CFP-OsUVR8b*. mCherry-H2B was used as a nuclear marker. Scale bars, 10 μm. Source data of Supplementary Figure 5d, g are provided as a Source Data file.

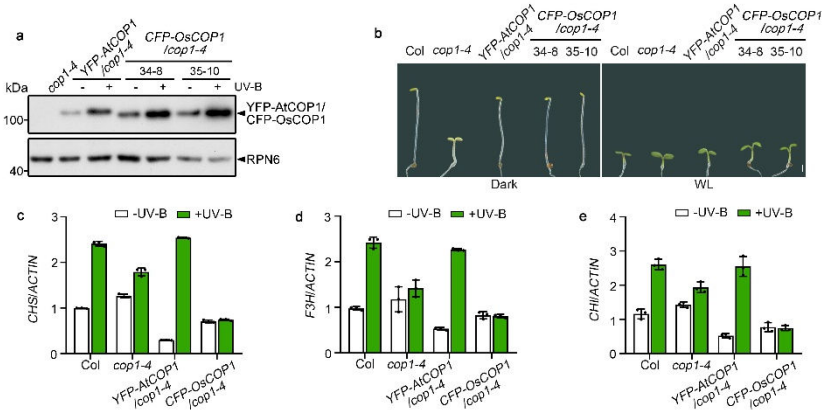

Supplementary Fig. 6 OsCOP1 plays a negative role in photomorphogenesis in transgenic Arabidopsis. a COP1 protein levels in 4-day-old *cop1-4*, *YFP-AtCOP1/cop1-4* and *CFP-OsCOP1/cop1-4* seedlings grown under −UV-B or +UV-B conditions. Immunoblot analysis was performed using anti-GFP antibodies. Anti-RPN6 was used as a loading control. **b** Representative images of 4-day-old Col-0, *cop1-4*, *YFP-AtCOP1/cop1-4* and *CFP-OsCOP1/cop1-4* seedlings grown in darkness or under WL conditions. Scale bar, 1 mm. **c–e** qRT-PCR analysis of the relative transcript levels of *CHS* (**c**), *F3H* (**d**) and *CHI* (**e**) in Col-0, *cop1-4*, *YFP-AtCOP1/cop1-4* and *CFP-OsCOP1/cop1-4* seedlings grown under −UV-B or +UV-B conditions. Transcript levels were normalized to *ACTIN*, with the transcript levels in Col-0 under −UV-B set to 1. Data are means ± SD; $n = 3$ biological replicates. Source data of Supplementary Figure 6a, c-e are provided as a Source Data file.

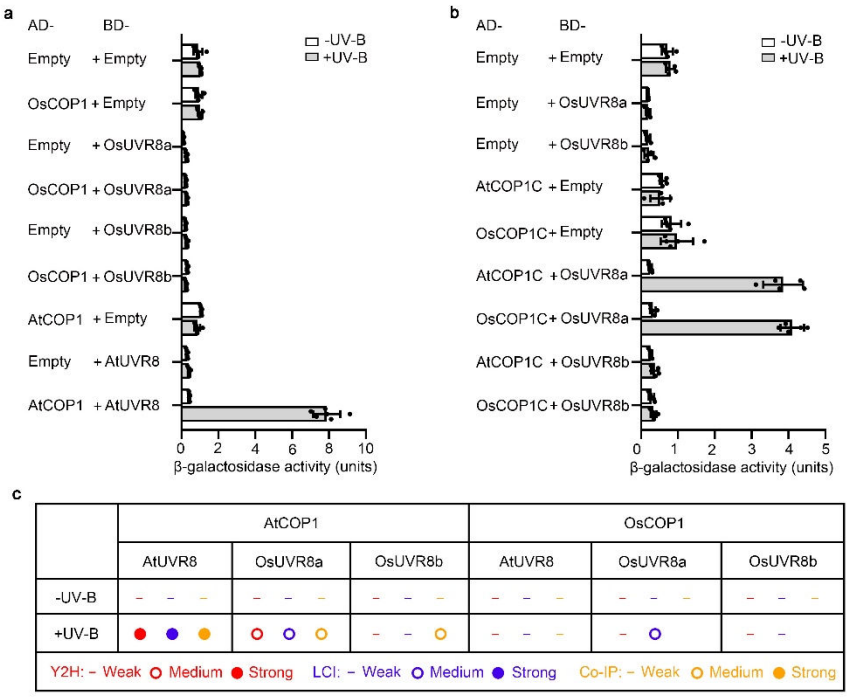

Supplementary Fig. 7 OsUVR8s and OsCOP1 do not directly interact in Y2H assays. a Quantitative Y2H assays showing the interaction of OsUVR8a and OsUVR8b with OsCOP1 in yeast cultures exposed to −UV-B or +UV-B conditions. AD, B42 activation domain; BD, LexA binding domain; Empty, empty vector. Data are means ± SD; $n = 6$ biological replicates. The *BD-AtUVR8* and *AD-AtCOP1* pair was used as a positive control. **b** Quantitative Y2H assays showing the interaction of OsUVR8a and OsUVR8b with AtCOP1C and OsCOP1C in yeast cultures exposed to −UV-B or +UV-B conditions. Data are means ± SD; $n = 5$ biological replicates. **c** Summary of the interaction patterns of UVR8–COP1. Results from Y2H, LCI and co-IP assays are shown in red, blue and yellow, respectively. The interaction intensities are denoted by a dash, open circles and filled circles, respectively. Source data of Supplementary Figure 7a, b are provided as a Source Data file.

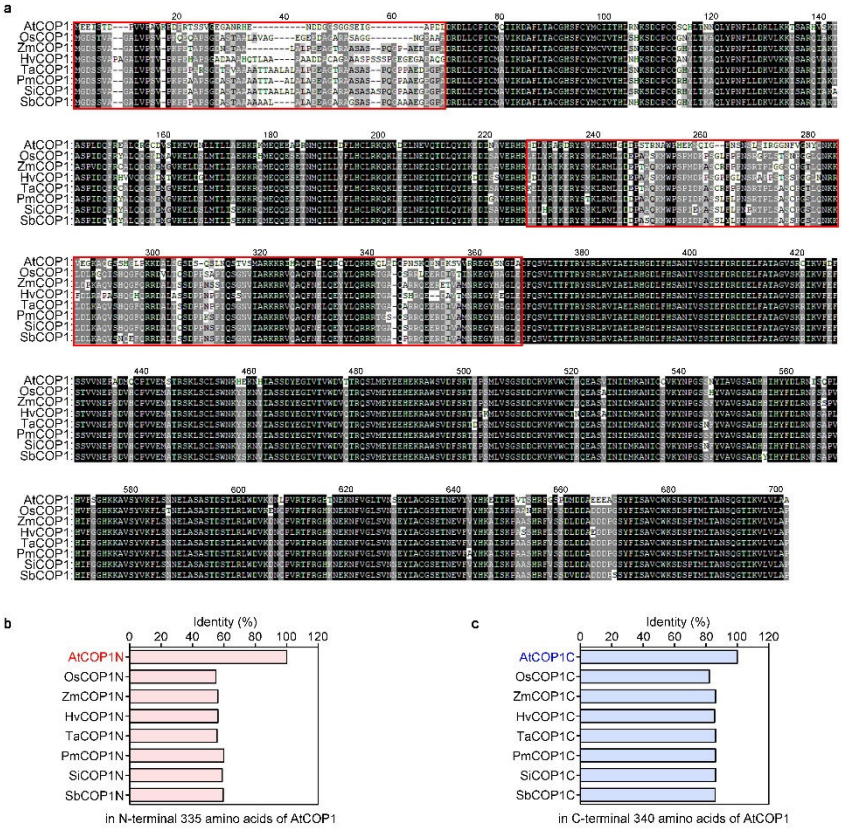

Supplementary Fig. 8 Monocot COP1 orthologs share sequence similarity with OsCOP1. a Multiple protein sequence alignment of AtCOP1 with OsCOP1, ZmCOP1, HvCOP1, TaCOP1, PmCOP1, SiCOP1 and SbCOP1. Identical residues are highlighted in black, and similar and different residues are highlighted in gray and white, respectively. The positions of less conserved regions in AtCOP1 and OsCOP1 are outlined in red. At, *Arabidopsis thaliana*; Os, *Oryza sativa*; Zm, *Zea mays*; Hv, *Hordeum vulgare*; Ta, *Triticum aestivum*; Pm, *Panicum miliaceum*; Si, *Setaria italica*; Sb, *Sorghum bicolor*. **b** Percentage protein sequence identity of the N terminus of AtCOP1 (first 335 amino acids) with the corresponding region in OsCOP1, ZmCOP1, HvCOP1, HvCOP1, TaCOP1, PmCOP1, SiCOP1 and SbCOP1. **c** Percentage protein sequence identity of the C terminus of AtCOP1 (last 340 amino acids) with the corresponding region in OsCOP1, ZmCOP1, HvCOP1, TaCOP1, PmCOP1, SiCOP1 and SbCOP1. Source data of Supplementary

Figure 8b, c are provided as a Source Data file.

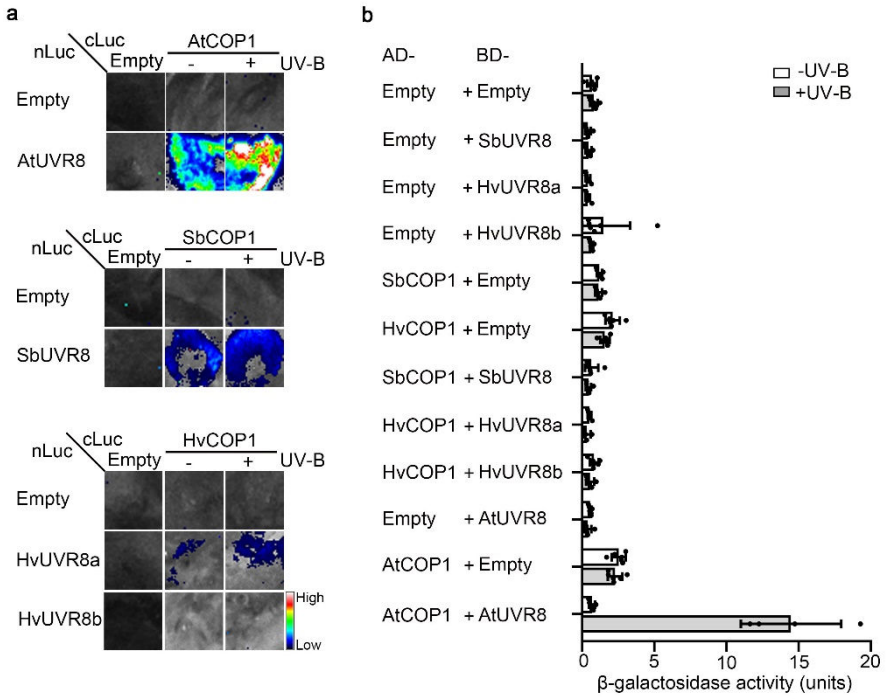

Supplementary Fig. 9 SbUVR8–SbCOP1 and HvUVR8s–HvCOP1 show weak interactions. a LCI assays showing the interaction between barley and sorghum COP1 with Arabidopsis UVR8 in *N. benthamiana*. *N. benthamiana* leaves were co-infiltrated with *SbUVR8-nLuc*, *HvUVR8a-nLuc*, *HvUVR8b-nLuc*, or *nLuc*, and *cLuc-SbCOP1*, *cLuc-HvCOP1* or *cLuc* as indicated. The *AtUVR8-nLuc* and *cLuc-AtCOP1* pair was used as a positive control. **b** Quantitative Y2H assays showing the interaction of Arabidopsis, barley and sorghum COP1 with their corresponding UVR8 in yeast cultures exposed to −UV-B or +UV-B conditions. AD, B42 activation domain; BD, LexA binding domain; Empty, empty vector. Data are means ± SD; $n \geqslant 4$ biological replicates. The *BD-AtUVR8* and *AD-AtCOP1* pair was used as a positive control. Source data of Supplementary Figure 9b are provided as a Source Data file.

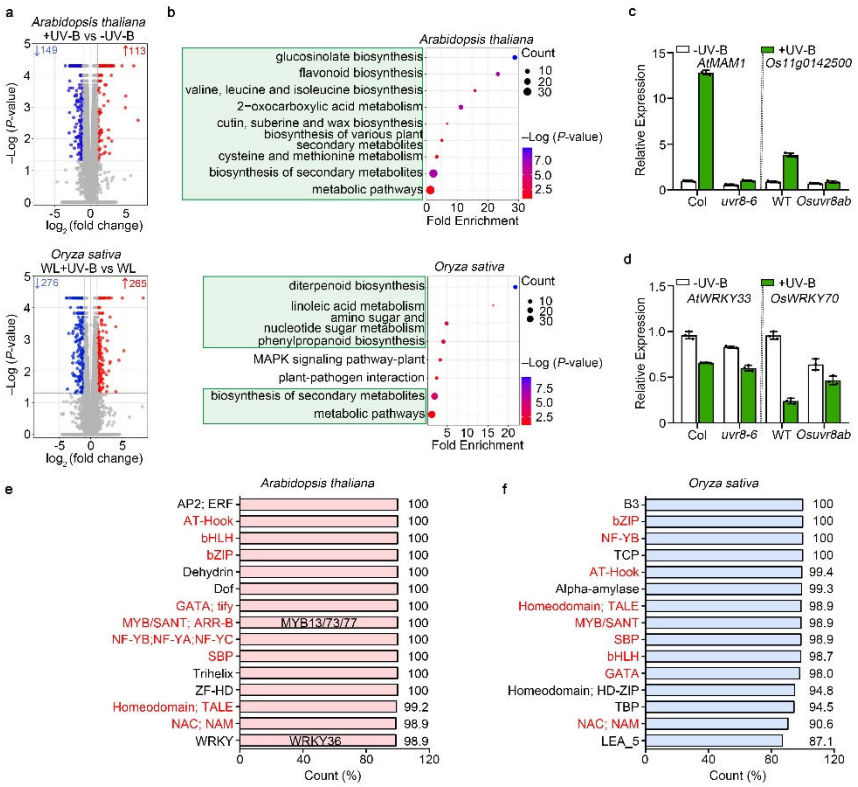

Supplementary Fig. 10 Distinct transcriptional responses to UV-B light in Arabidopsis and rice. a Transcriptome analysis of gene expression regulated by UV-B light in Arabidopsis (top) and rice (bottom). **b** KEGG pathway enrichment analysis for biological processes regulated by UV-B light in Arabidopsis (top) and rice (bottom). **c**, **d** qRT-PCR analysis of the relative transcript levels of *AtMAM1* and *AtWRKY33* in Col-0 and *uvr8-6* seedlings grown under −UV-B or +UV-B conditions. Transcript levels were normalized to *ACTIN*, with transcript levels in Col-0 under −UV-B set to 1. qRT-PCR analysis of the relative transcript levels of Os11g0142500 and *OsWRKY70* in WT DJ and *Osuvr8ab* seedlings grown under WL or WL+UV-B conditions. Transcript levels were normalized to *UBQ*, with transcript levels in WT DJ under WL set to 1. Data are means ± SD. $n = 3$ biological replicates. **e, f** Prediction of transcription factors potentially involved in the regulation of UV-B responsive gene expression in Arabidopsis (**e**) and rice (**f**). Conserved transcription factors in both species are indicated in red. Count

(%) represents the percentage of differentially expressed genes to which promoter the transcription factor can bind out of all differentially expressed genes. Source data of Supplementary Figure 10c-f are provided as a Source Data file.

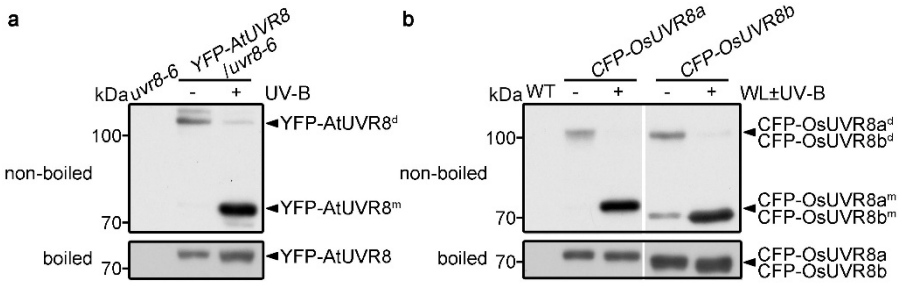

Supplementary Fig. 11 Conformation of AtUVR8, OsUVR8a and OsUVR8b. a, b Conformation of YFP-AtUVR8 in 4-day-old Arabidopsis *YFP-AtUVR8/uvr8-6* seedlings grown under −UV-B or +UV-B conditions (**a**) and 10-day-old CFP-OsUVR8a and CFP-OsUVR8b in rice *CFP-OsUVR8a* and *CFP-OsUVR8b* seedlings grown under WL or WL+UV-B conditions (**b**). Total proteins were separated by SDS-PAGE with or without prior heat denaturation, followed by immunoblot analysis using anti-GFP antibodies. d, dimer; m, monomer. Source data are provided as a Source Data file.

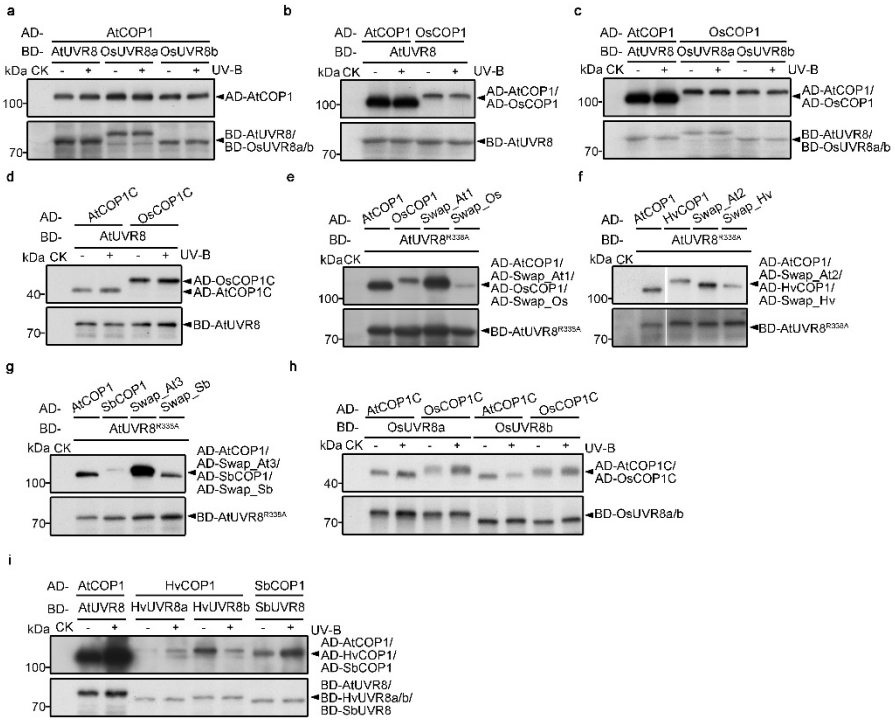

Supplementary Fig. 12 Detection of BD-fusion and AD-fusion proteins in yeast for the quantitative Y2H assays. a Related to **Fig. 3f**. **b** Related to **Fig. 5j**. **c** Related to **Supplementary Fig. 7a**. **d** Related to **Fig. 6b**. **e** Related to **Fig. 6e**. **f** Related to **Fig. 6i**. **g** Related to **Fig. 6j**. **h** Related to **Supplementary Fig. 7b**. **i** Related to **Supplementary Fig. 9b**. Anti-LexA and anti-HA antibodies were used to detect BD-fusion and AD-fusion proteins respectively. Source data are provided as a Source Data file.

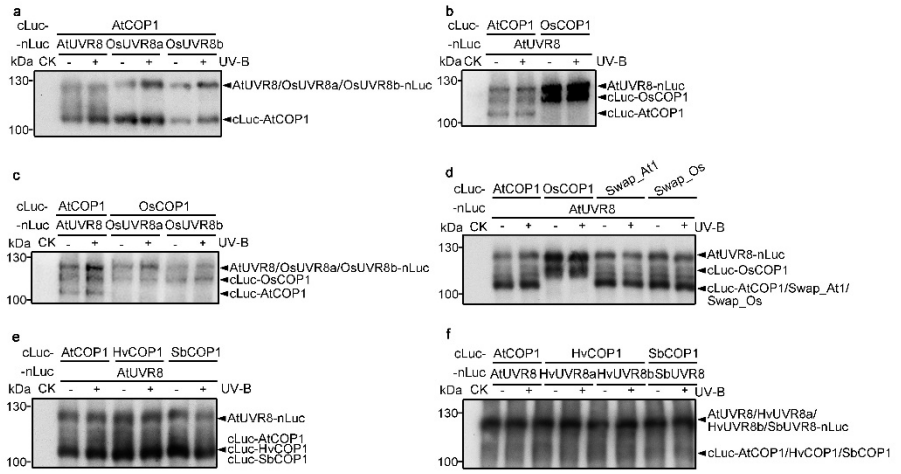

Supplementary Fig. 13 Detection of cLuc-fusion and nLuc-fusion proteins in *N. benthamiana* leaves for LCI assays. a Related to **Fig. 3g**. **b** Related to **Fig. 5k**. **c** Related to **Fig. 6a**. **d** Related to **Fig. 6d**. **e** Related to **Fig. 6g**. **f** Related to **Supplementary Fig. 9a**. Anti-Luc antibodies were used to detect cLuc-fusion and nLuc-fusion proteins. Source data are provided as a Source Data file.